Journal of Sol-Gel Science and Technology (2019) 89:602–615
https://doi.org/10.1007/s10971-018-4870-0

ORIGINAL PAPER: SOL–GEL AND HYBRID MATERIALS FOR ENERGY, ENVIRONMENT AND BUILDING APPLICATIONS

Synthesis of phosphorylated raw sawdust for the removal of toxic metal ions from aqueous medium: Adsorption mechanism for clean approach

Mosaed Saud Alhumaimess[1] · Ibrahim Hotan Alsohaimi[1] · Ayoub Abdullah Alqadami[2] · Mahmoud Mohamed Kamel[1] · Mu. Naushad[2] · Tansir Ahamad[2] · Hamed Alshammari[3]

Received: 9 May 2018 / Accepted: 29 October 2018 / Published online: 12 November 2018

Abstract

In this work, phosphorus oxychloride was grafted onto the surface of raw sawdust (RSD) particles to get effective adsorbent for capturing Cd(II), Cr(III), and Pb(II) metal ions from aqueous medium. Phosphorylated raw sawdust (RSD@P) was characterized by FTIR, TGA, SEM-EDX, TEM, BET, and XPS analyses. Various experimental conditions of adsorption viz. pH, contact time, temperature, and initial concentration were optimized. The adsorption behavior of RSD@P concerning adsorption kinetics, isotherms and thermodynamics was also studied. The values of qe for Cd(II), Cr(III), and Pb(II) metal ions onto RSD@P was found to be 244.3, 325, and 217 mg/g, respectively at 298 K according to monolayer Langmuir adsorption. The adsorption kinetics data revealed that Cd(II), Cr(III), and Pb(II) metal ions were well fitted to pseudo-second-order kinetic model. The thermodynamic results demonstrated that adsorption was spontaneous and exothermic. The mechanisms of interactions was also discussed for the adsorption of Cd(II), Cr(III), and Pb(II) metal ions over RSD@P. The obtained results showed that RSD@P was an auspicious adsorbent which showed outstanding reusability for the removal of metal ions from aqueous medium.

Graphical Abstract

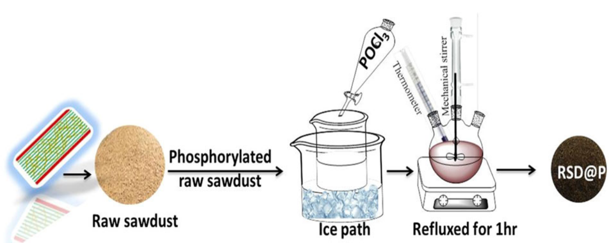

Electronic supplementary material The online version of this article (https://doi.org/10.1007/s10971-018-4870-0) contains supplementary material, which is available to authorized users.

✉ Mu. Naushad
mnaushad@ksu.edu.sa

[1] Department of Chemistry, College of Science, Jouf University, Sakaka-2014, Saudi Arabia

[2] Department of Chemistry, College of Science, King Saud University, Bld#5, Riyadh 11451, Saudi Arabia

[3] Faculty of Science, Department of Chemistry, University of Hail, Hail 81451, Saudi Arabia

Highlights

- Crosslinked phosphorylated raw sawdust (RSD@P) was prepared.
- The material (RSD@P) was used for the removal of Cd(II), Cr(III), and Pb(II) from aqueous medium.
- Adsorption of all metal ions onto RSD@P was rapid, spontaneous, and exothermic.
- The values of qe for Cd(II), Cr(III), and Pb(II) was 244.3, 325, and 217 mg/g, respectively.
- The RSD@P was regenerated by simply washing with 0.1 M HCl solution.

Keywords Phosphorylated sawdust · Adsorption · Toxic metals · Adsorption models

1 Introduction

Obtaining pure water is a major concern and great demand for humane life because it is continuously polluted by toxic heavy metals which leads to serious environmental problems to many forms of life [1–3]. Aqueous wastes of many industries, modern urbanization, mining and dissolution from the associated geologic formations are main sources of water contamination by heavy metals [4, 5]. Lead, cadmium and chromium are main metals whose existence in aqueous solutions leads to many health problems [6–8]. So, it is one of the most important challenges to the scientist to remove these toxic metal ions from aqueous environment [9, 10]. Several trials and efforts have been demonstrated using various treatments such as adsorption, ion exchange, reverse osmosis, chemical precipitation, electrochemical removal, and biosorption [11–14].

Adsorption has considerably been used because of its effectiveness and economic visibility. Lead, cadmium, and chromium has been removed by using several adsorbents [7, 15–17]. In recent years, the search for economical and convenient adsorbents based on naturally found materials and/or their modification has been increasingly demanded. Sawdust, as one of the alternative absorbent materials has been particularly used for the exclusion of various metal ions from aqueous medium [5, 18, 19]. Wood sawdust is widely available as a waste of carpenter workshops and its chemical composition contains cellulose, hemicelluloses, and lignin. Hence, we attempted to modify the wood sawdust to increase its efficiency for heavy metal removal. The modification process was based on increasing the uptake capacity through introducing phosphate as ion exchange groups. Recently, the oak tree sawdust has been modified by phosphate groups using phosphoric acid for the removal of lead ions [20]. However, our modification involves a new procedure for phosphorylation the hydroxyl groups on wood sawdust components using phosphorous oxychloride. The modified sawdust was subjected to different analyses and its applications for the adsorptive removal of lead, cadmium and chromium was also examined.

2 Experimental

2.1 Materials and chemicals

The chemicals and reagents which were used here were of analytical reagent grade. HNO_3 and NaOH were procured from Merck, Germany. $Cr(NO_3)_3$, $Pb(NO_3)_2$, $Cd(NO_3)_2.4H_2O$, and HCl were purchased from BDH, England. Phosphorus oxychloride ($POCl_3$), Triethylamine (HPLC grade; 99%) and Tetrahydrofuran were obtained from Scharlau, Spain and Lobal Chemic laboratory Reagent and Fine Chemicals, India, respectively.

2.2 Synthesis of crosslinked phosphorylated raw sawdust

Sawdust was obtained from carpentry workshops and its phosphorylation reaction was carried out by sol–gel method as follows: 3 g of sawdust was added to a mixture containing 10 mL of tetrahydrofuran (THF) and 5 mL of triethylamine (TEA). The mixture was cooled in ice bath with a dropwise addition of 15 mL phosphorus oxychloride to the mixture. The mixture was then refluxed for 1 h. The attained yield was repetitively washed with hot distilled water and dried at 70 °C for 12 h. The obtained product of phosphorylated raw sawdust was designated as (RSD@P).

2.3 Adsorption studies

The batch mode experiments were done to test the adsorption of Cd(II), Cr(III), and Pb(II) onto RSD@P. Typically, 15 mg of RSD@P adsorbent was taken in 100 mL conical flask having 25 mL of 25 mg/L from each metal ion separately at 298 K and shaken at 100 rpm for 24 h. After a fixed time interval, an aliquot of the sample was withdrawn from the flask and the concentration of each metal ion in the supernatant was determined by AAS. The % adsorption and q_e at equilibrium was determined as:

$$\text{Adsorption }\% = \frac{C_o - C_e}{C_o} \times 100 \quad (1)$$

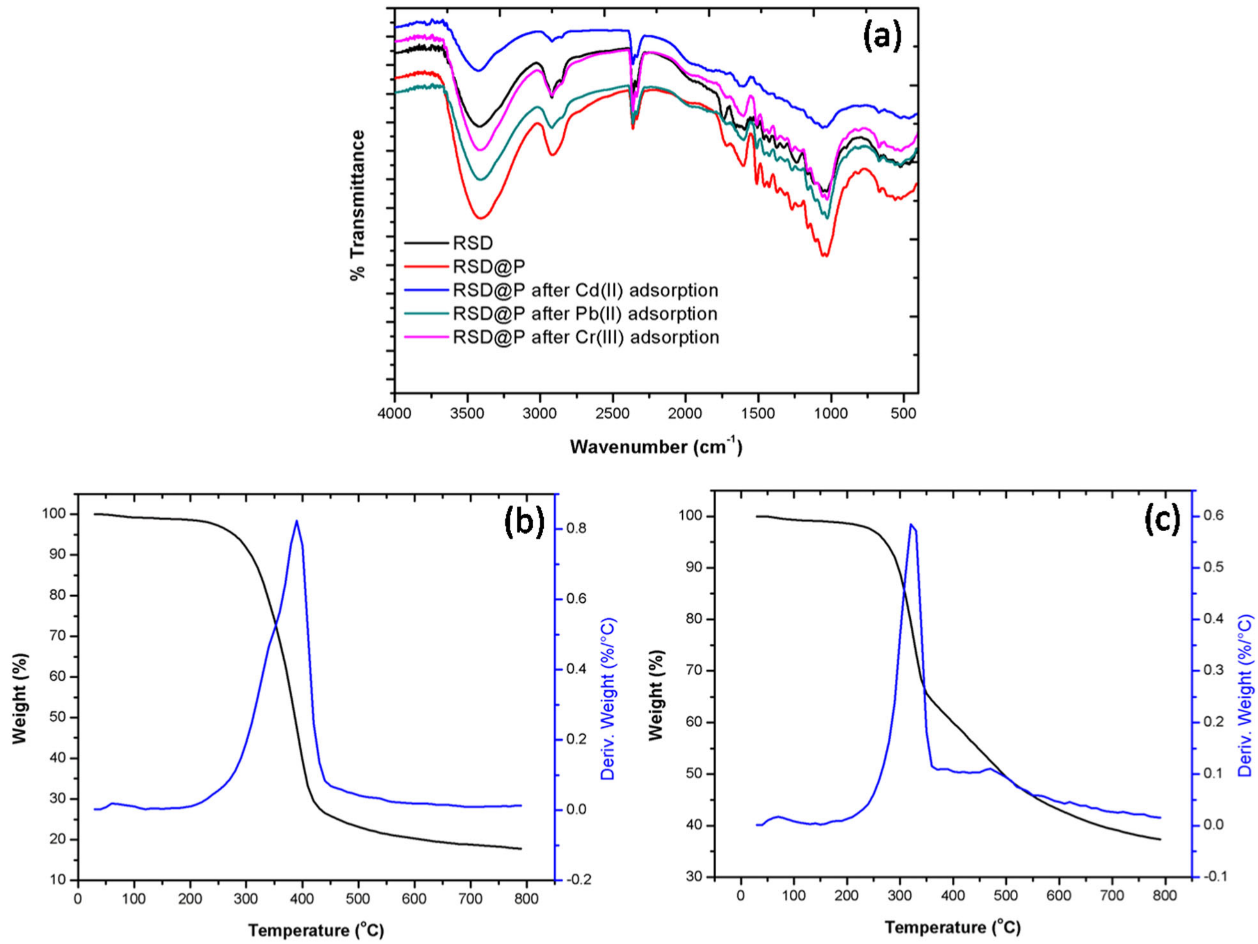

Fig. 1 FT-IR spectra of **a** RSD and RSD@P before and after metals adsorption onto RSD@P **b** TGA-DTA curves corresponding to RSD **c** and RSD@P

$$q_e(\mathrm{mg/g}) = (C_o - C_e)\frac{\mathrm{V}}{\mathrm{m}} \quad (2)$$

The effect of pH on the removal of Cd(II), Cr(III), and Pb (II) metal ions using RSD@P was examined in the pH range of 2 to 10. The effect of contact time on the adsorption of these metals was done in the time range of 1 to 1440 min. Moreover, the effect of initial concentration of the current metal ion adsorption was investigated for diverse C_o range: 25 to 300 mg/L at different temperatures; 25 to 45 °C.

Desorption experiments were also investigated in batch method. 15 mg of RSD@P was added to 25 mL of 25 mg/L each of metal ions solution under agitation speed of 180 min at 298 K. After 180 min, Cr(III), Cd(II), and Pb(II) metal ions saturated RSD@P sample was isolated from aqueous solution through filtration and it was treated with 25 mL 0.1 M HCl to elute Cd(II), Cr(III), and Pb(II) metal ions. After 180 min, the RSD@P sample was separated from the solution phase and the concentration of metal ions in the solution phase was evaluated using AAS and the percentage of desorption of these metal ions were found as:

$$\text{Desorption}\,\% = \frac{\text{Conc. of metal ions desorbed by eluent}}{\text{Initial conc.of metal ions adsaorbed on RSD@P}} \times 100 \quad (3)$$

We also tried 0.1 M HNO_3 solutions for the elution of these metal ions using the same procedure mentioned above.

3 Results and discussion

3.1 Characterization of RSD and RSD@P

The RSD and RSD@P samples were characterized by SEM-EDX, TEM, FTIR, TGA-DTA, XRD, BET, and XPS and details are given in Text S1 (Supplementary material). Figure 1a shows the FTIR spectra of RSD and RSD@P (before and after adsorption). The strong peak at ~3423 cm^{-1} and ~1662 cm^{-1} could be accredited to O–H vibrations signifying the presence of cellulose, hemicellulose and lignin. Peaks at 2918 and 2845 were attributed to C–H stretching vibration of aliphatic compound [21]. The peak at 1740 cm^{-1} and between 1589 – 1503 cm^{-1} were allotted to aliphatic carbonyl of xylan hemicellulose, and aromatic rings from lignin, respectively [22, 23]. Also, Fig. 1a showed the finger print region peaks of cellulose, hemicellulose and lignin in the raw sawdust between 1100 and 1800 cm^{-1}. Peaks at 1370 cm^{-1} and 1446 cm^{-1} allotted to the C–H stretching vibration of hemicellulose and the C–H bending of the cellulose and lignin, respectively [24]. The peak at 1232 cm^{-1} was assigned to C–O stretching band indicating the presence of hemicellulose [25]. The peaks at 1158 and 1048 cm^{-1} were assigned to a C–O stretching band of C–O–H group and C–O–C group in the anhydroglucose ring, respectively. After modification of RSD by $POCl_3$' there was a little change in figure. The band in the 1100 to 1200 cm^{-1} region presented in the spectra for P=O group. The peak in the region between 700 to 850 cm^{-1} was probably allotted to the P–O–C bond. The peak at 2360 cm^{-1} was ascribed to P–H group [26–28].

It can be clearly seen that some changes were noticed in the FT-IR spectra after adsorption of Cd(II), Cr(III) and Pb (II) metal ions onto RSD@P. The decrease and changes in the FT-IR spectra was observed at the peak between 1100 to 1200 cm^{-1} and the bands of 1176–1040 cm^{-1} after Cd(II), Cr(III), and Pb(II) metal ions adsorption onto RSD@P, the P=O structures at between 1100 to 1200 cm^{-1} was shifted to low. These results suggested that the adsorption between these cations and adsorbent surface was governed by the electrostatic interaction.

TGA analysis was accomplished to define the thermal stability of both RDS and RSD@P under inert N_2 atmosphere. Figure 1b, c shows the TGA with the first derivative of RDS and RSD@P. As can be seen, the thermal degradation of the RDS (Fig. 1b) mainly occurred at temperatures between 220 and 420 °C and about 73% weight loss was observed. At 150°C, 2% weight loss was noted which assigned to the removal of adsorbed water and residual solvent from the RSD sample [29, 30]. So, the thermal decomposition of RDS was achieved in one step. The observed weight loss was ascribed to the degradation of hemicellulose, cellulose and degradation of lignin [31]. For the RSD@P (Fig. 1c), there are two steps; the first step took place in the temperature range 250–375 °C. A weight loss of about 48% was noticed due to the breakdown of hemicellulose and cellulose and degradation of lignin. In the second step, the 10% weight loss observed in the range of temperature between 400–800 °C rationally related to the degradation of residual of lignin and phosphoryl group. These two steps indicated the successful modification of RSD by $POCl_3$. The BET surface area and the total pore volume of RSD@P were higher than that of untreated RSD and found to be 14.56 m^2/g and 0.0090 cm^3/g, respectively.

The morphologies of RSD, RSD@P before and after adsorption onto RSD@P are shown in Fig. 2. Smooth morphology and fewer pores were available on the sawdust surface (Fig. 2a). After modification with phosphorus oxychloride ($POCl_3$), large pores or cavities and channels were observed in the RSD@P (Fig. 2b). After the adsorption of Cd(II), Cr(III), and Pb(II), the surface morphology was changed which might be due to the interaction of these metal ions with the functional groups of RSD@P (Fig. 2c–e). The pores were completely occupied by these metal ions leading to a formation of rough and non-uniform covering over RSD@P surface. These morphological changes confirmed the adsorption of these heavy metal ions onto RSD@P surface.

TEM images of RSD are given in Fig. 3a. The morphology of untreated RSD presented heterogeneous and aggregated surface. The porosity of RSD particles was approximately 42 nm (Fig. 3a, inset). The particle size of RSD particles was 22 nm (Fig. 3b). After modification with $POCl_3$ (Fig. 3c), a high porosity was observed (Fig. 3c, inset) and the particle size of RSD@P became 24 nm (Fig. 3d). Also after modified with $POCl_3$, the RSD particles coated by a layer of $POCl_3$ (Fig. 3c). The elemental analysis of RSD and RSD@P were performed by EDX analysis (Table 1 and Fig. 4). Untreated RSD spectrum (Fig. 4a) displayed only C and O peaks, while RSD@P spectrum showed the presence of C and O, as well as new peaks of P and Cl (Fig. 4b). This result confirmed the successful modification of RSD by $POCl_3$. The results of elemental composition of RSD@P after adsorption of Cd(II), Cr(III), and Pb(II) showed clearly the presence of Cd(II), Cr(III), and Pb(II) in the structure of the RSD@P.

Figure 5 shows the XPS of RSD and RSD@P. Figure 5a shows two peaks at 284.8 and 530.5 assigning to C 1 s and O 1 s peaks, respectively for RSD; the RSD@P spectrum shows two additional peaks at 134.3 and 206 eV which might be due to P 2p and C 1 s, respectively [32]. The high-resolution spectrum of C 1 s, O 1 s and P 2p is shown in Fig. 5b. Peaks at 284.6.0, 285.2, 286.3, 286.5 and 288.1 eV were assigned to C–C, C–OH, C–O, C=O and O=C–O, respectively [33]. On the other hand, peaks at 529.9, 531.3, 532.5, and 534.5 eV corresponded to O=P, O–C, O=C and O=C–O, respectively (Fig. 5c). The peak at 134.3 eV corresponded to P 2p (Fig. 5d) [34]. The presence of P and Cl peaks in RSD@P spectrum also confirmed the successful modification of RSD surface by $POCl_3$.

3.2 Adsorption performance

The pH is one of the most essential parameters which effects the surface charge of adsorbent material and metal ion speciation in aqueous solution [35–37]. The effect of solution pH on adsorption process was examined in the pH

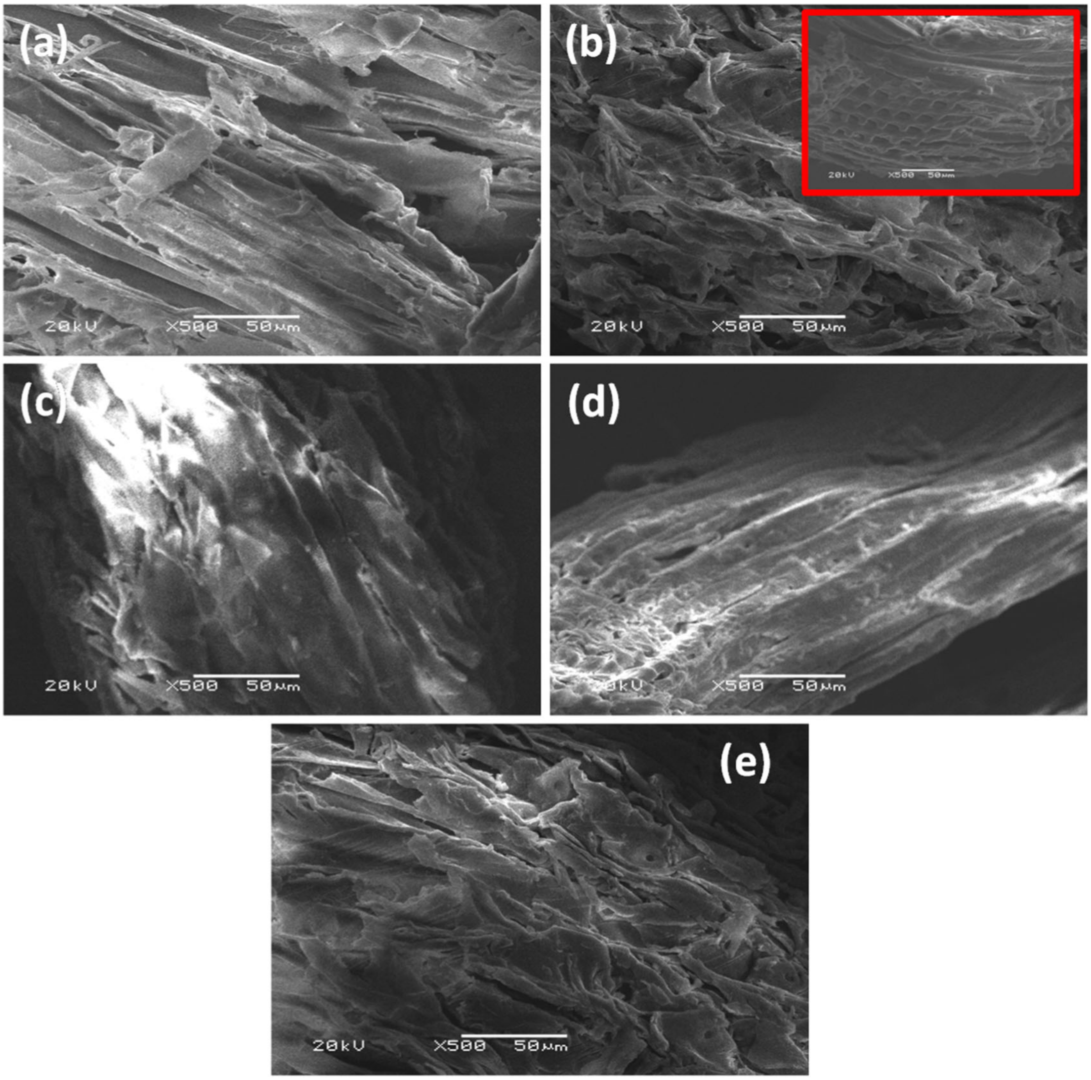

Fig. 2 SEM images of **a** untreated RSD, **b** RSD@P **c**–**e** RSD@P after adsorption of Cd(II), Cr(III) and Pb(II) metal ions

range of 2–10. Figure 6a displays the effect of pH on the adsorption of Cd(II), Cr(III), and Pb(II) metal ions adsorbed onto RSD@P and rest parameters were kept constants (contact time 1440 min, RSD@P dose 15 mg, temperature 25 °C). The results showed that qe for Pb(II) was increased with increasing the pH from 2.0 to 5.8, then it started to decrease. The qe was 3.7 $mg\ g^{-1}$ at pH 2 and increased up to 56.7 $mg\ g^{-1}$ at pH 5.8. In the case of Cd(II) and Cr(III), the qe was increased until pH 7, then it started to decrease. The qe was 4.6 $mg\ g^{-1}$ and 6.1 $mg\ g^{-1}$ at pH 2 which increased up to 56.2 and 57.8 $mg\ g^{-1}$ at pH 7 for Cd(II) and Cr(III), respectively. The adsorption of these metal ions was decreased at higher pH which was due to the formation of metal hydroxides [38]. At low pH, the adsorptive removal of these metal ions was low which may be due to the high concentration of H^+ in the acidic medium, so protonation of the active sites of RSD@P dominated over the adsorption process. As the pH of the solution increases (<7), number of negatively charged sites increased, so that adsorption of these metal ions was increased.

Effect of time on the adsorbed amount of Cd(II), Cr(III), and Pb(II) metal ions using RSD@P adsorbent was studied in the range of 5–240 min as shown in Fig. 6b. It was noted that qe of Cd(II), Cr(III), and Pb(II) metal ions was increased with increasing the contact time until the equilibrium was attained (180 min). Adsorption rate was gradually increased up to 180 min for all metal ions. The maximum adsorption capacity for Cd(II), Cr(III), and Pb(II) metal ions was 33.75, 34.40, and 32.7 mg/g, respectively, hence 180 min was enough to reach to equilibrium.

Figure 7 shows the effect of initial concentration of Cd (II), Cr(III), and Pb(II) metal ions (25–300 mg/L) on adsorption at different temperatures (25, 35, and 45 °C). The q_e of all metal ions was increased with increasing the

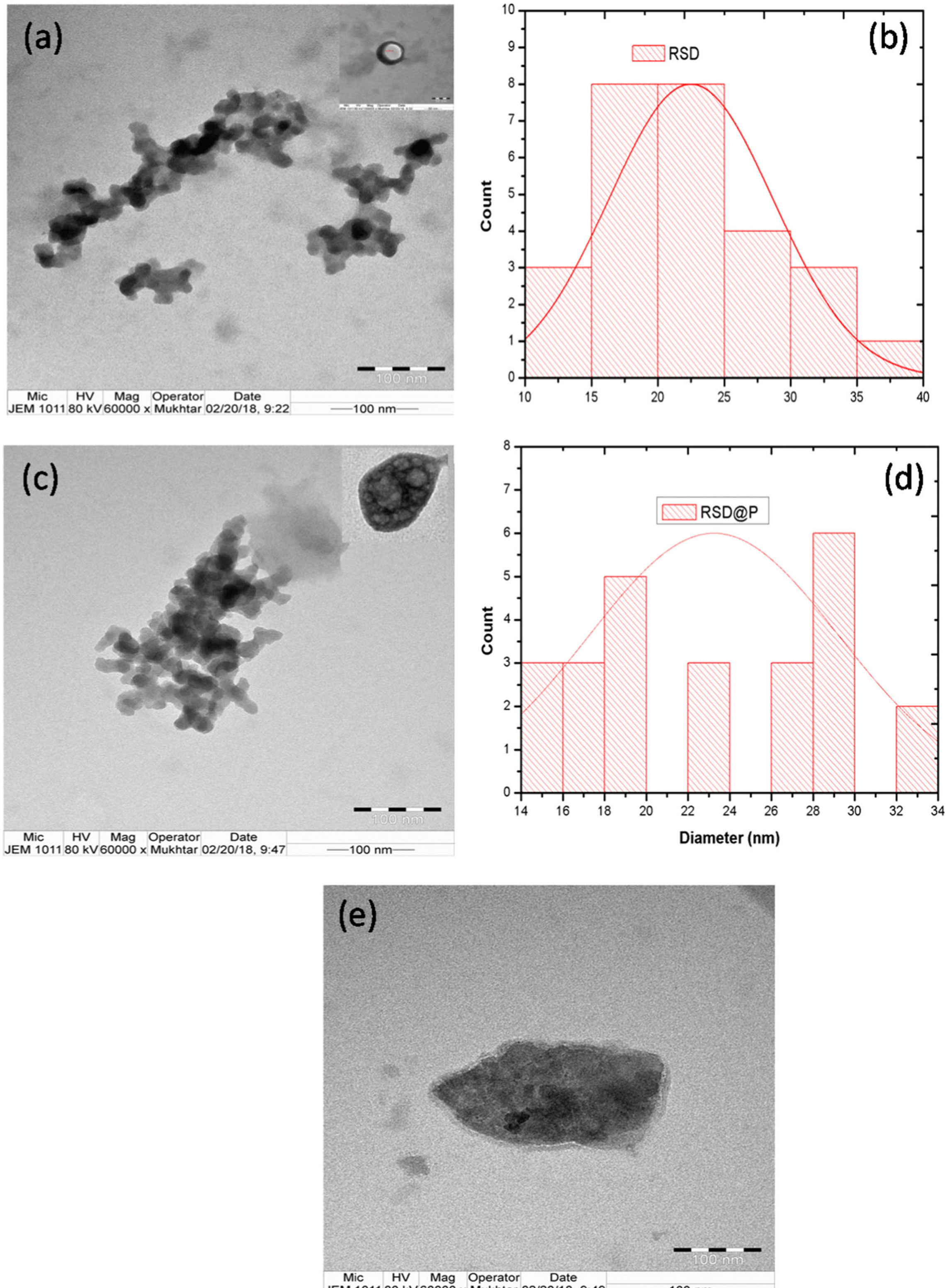

Fig. 3 TEM images and particle size distribution of untreated RSD **a**, **b** and RSD@P **c**–**e**, respectively

Table 1 Elemental analysis of RSD, RSD@P, and saturated RSD@P after the adsorption of heavy metals

Sample	Elemental content (%)						
	C	O	P	Cl	Cd	Cr	Pb
RSD	51.30	48.70	–	–	–	–	–
RSD@P	48.57	50.24	0.65	0.54	–	–	–
RSD@P + Cd(II)	52.23	45.54	0.46	0.37	1.41	–	–
RSD@P + Pb(II)	51.53	44.60	0.73	0.50	–	–	2.64
RSD@P + Cr(III)	53.93	44.63	0.65	0.47	–	0.32	–

initial metal ion concentration, while the percent adsorption of these metal ions displayed the opposite trend. Once, the initial concentration of Cd(II), Cr(III), and Pb(II) metal ions was increased from 25 to 300 mg/L, the q_e was increased from 28.75 to 162.50 mg g^{-1}, 29.37 to 213.07 mg g^{-1}, and 28.37 to 148.88.50 mg g^{-1} at 25 °C, respectively. The increase in the adsorption capacity with increasing initial metal concentrations could be attributed due to the accessibility of vacant sites for metal binding [39–41]. It can be concluded that RSD@P is able to bind Cd(II), Cr(III), and

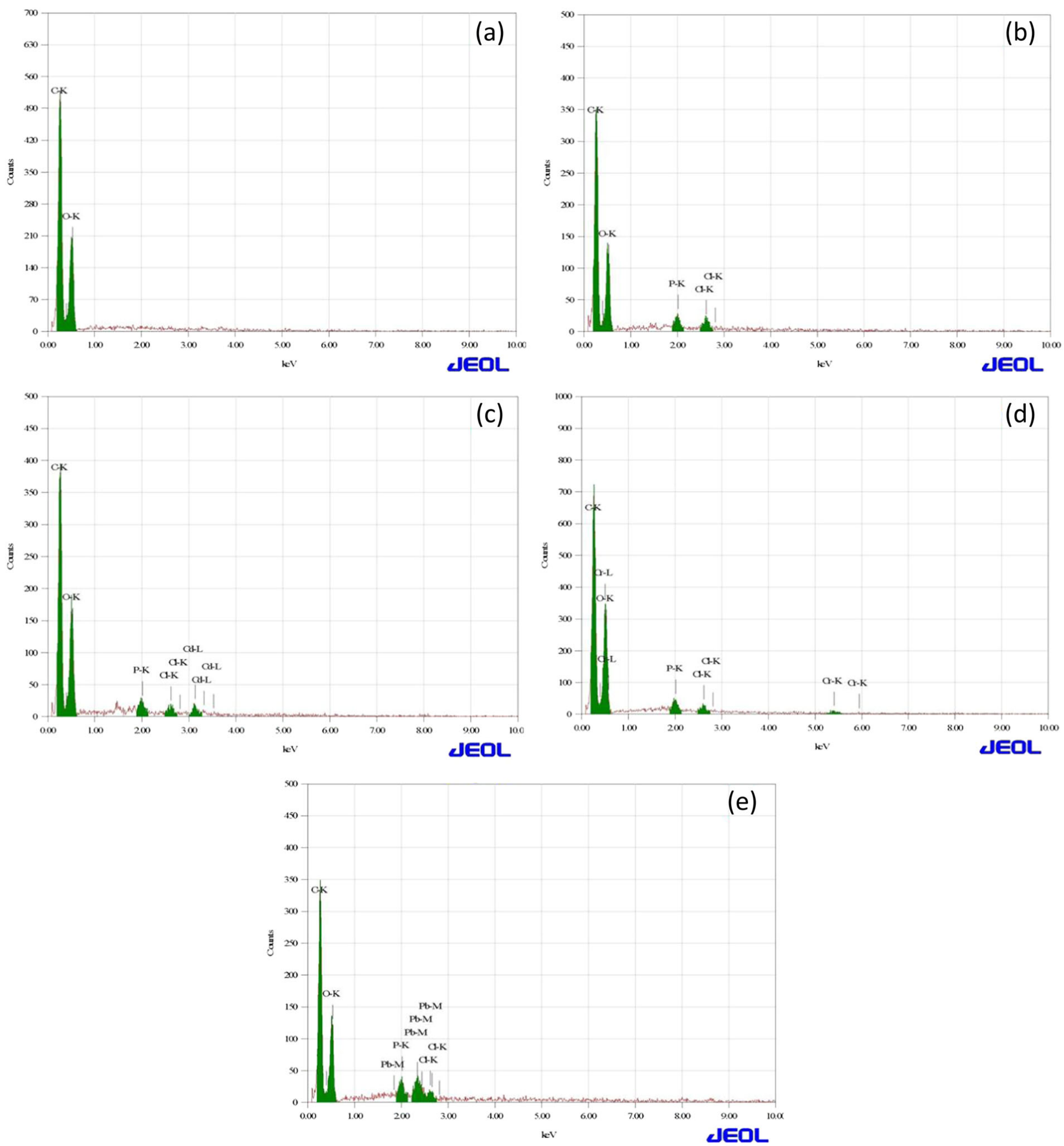

Fig. 4 EDX images of **a** untreated RSD, **b** RSD@P **c**–**e** RSD@P after adsorption of Cd(II), Cr(III), and Pb(II) metal ions

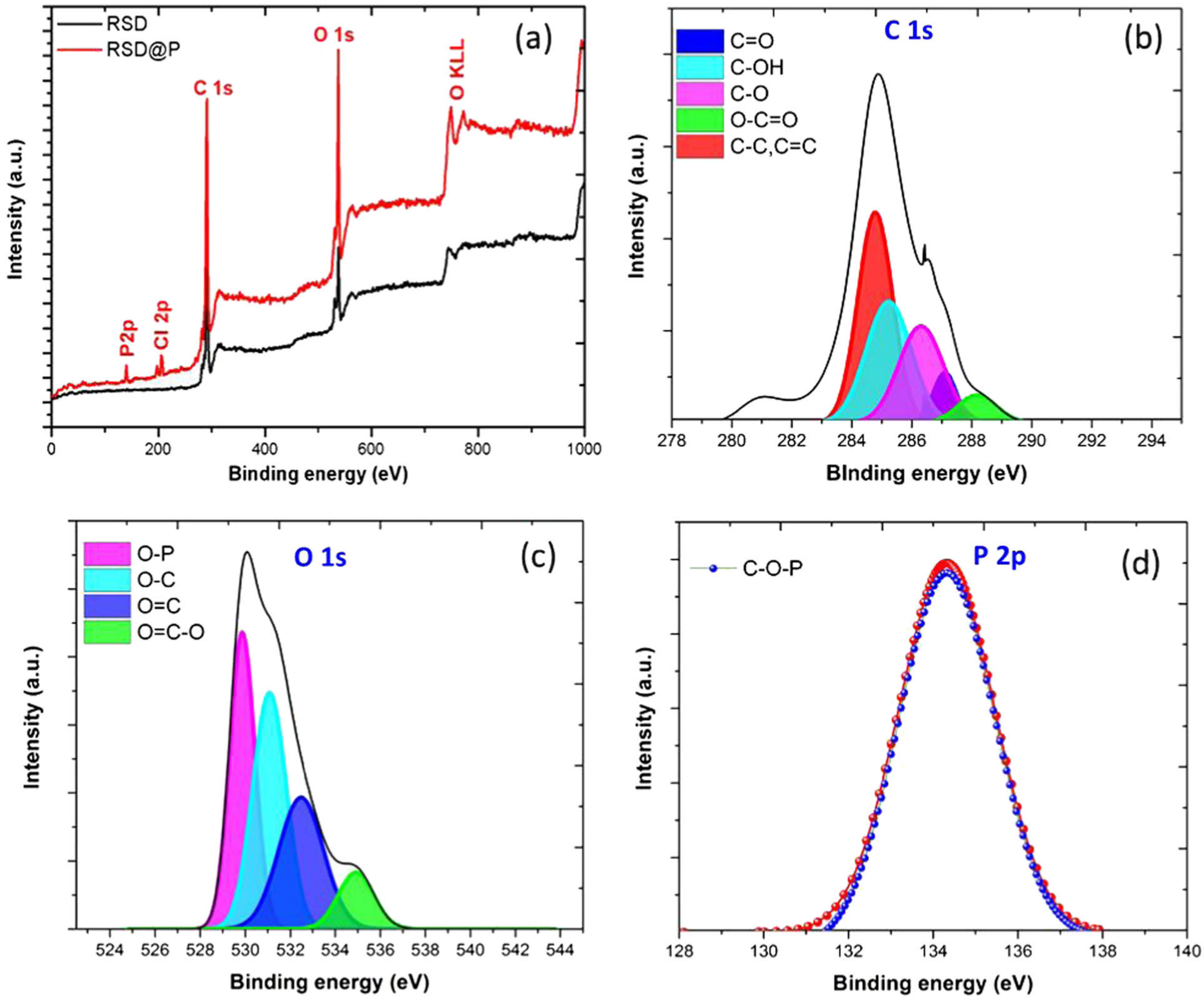

Fig. 5 **a** X-ray photoelectron spectroscopic images of RSD and RSD@P; High-resolution XPS spectrum for **b** C 1 s, **c** O 1 s, **d** P 2p

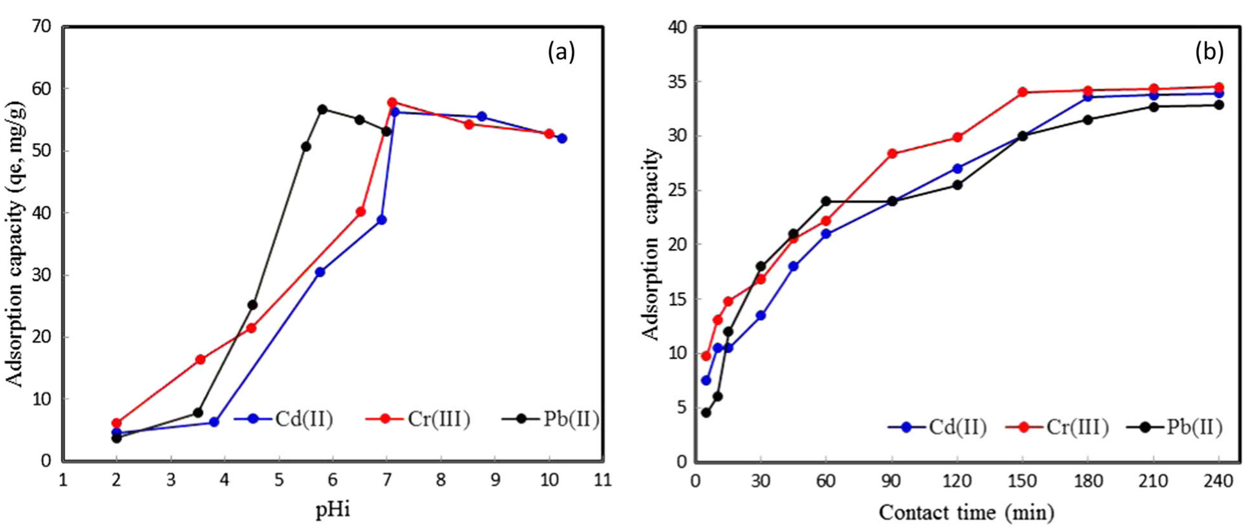

Fig. 6 Removal of Cd(II), Cr(III), and Pb(II) metal ions using RSD@P at different **a** pH and **b** time

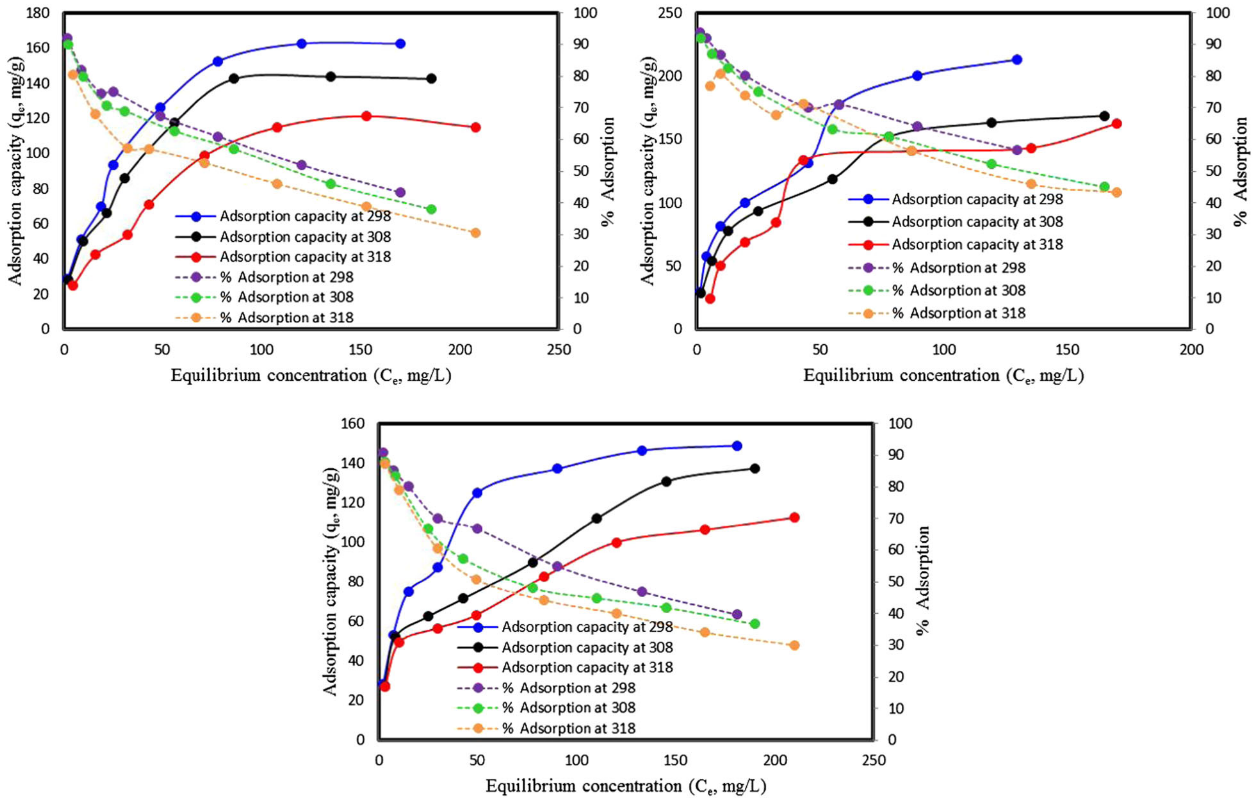

Fig. 7 Effect of concentration on the adsorption capacity of Cd(II), Cr(III), and Pb(II) using RSD@P at different temperatures

Table 2 Isotherm parameters for the adsorption of Cd(II), Cr(III), and Pb(II) metal ions onto RSD@P

Metal ions	Temperature (K)	q_m, exp. (mg/g)	Langmuir isotherm			Freundlich isotherm		
			q_m, cal (mg/g)	K_L	R^2	K_f (mg/g)(L/mg)1/n	N	R^2
Cr(III)	298	284.1	325.0	0.042	0.933	41.23	2.46	0.973
	308	225.0	245.4	0.051	0.958	39.82	2.84	0.972
	318	216.66	244.8	0.030	0.928	26.88	2.44	0.983
Cd(II)	298	284.1	244.3	0.042	0.959	38.32	2.89	0.923
	308	190.0	217.9	0.041	0.945	35.48	2.98	0.896
	318	153.33	198.8	0.024	0.950	21.54	2.55	0.912
Pb(II)	298	198.51	217.0	0.057	0.965	41.74	3.17	0.986
	308	183.33	201.2	0.024	0.857	24.79	2.62	0.971
	318	150.0	157.2	0.038	0.852	25.66	3.01	0.973

Pb(II) metal ions over a wide range of concentrations. Moreover, the qe was decreased with increasing the temperature from 25 to 45 °C, confirmed the exothermic nature of adsorption process [33].

3.3 Adsorption isotherms

The behavior of Cd(II), Cr(III), and Pb(II) metal ion adsorption, as well as their interaction onto RSD@P was performed using Freundlich [42] and Langmuir models [43] and the information concerning the models is given in Supplementary Information (Text S2). The isotherm data concerning the adsorption of these metal ions on RSD@P is presented in Table 2. On the basis of the correlation coefficient (R^2) values, Freundlich isotherm showed a better fit of experimental data than that of Langmuir isotherm models at all temperatures (except Cd(II)) which showed the existence of multilayer surface condition (Fig. 8) [44]. It can be observed that values of K_f of Freundlich isotherm constants were decreased with increasing temperature from 298 to 318 K, implying that the adsorption was exothermic in nature. The maximum calculated monolayer adsorption

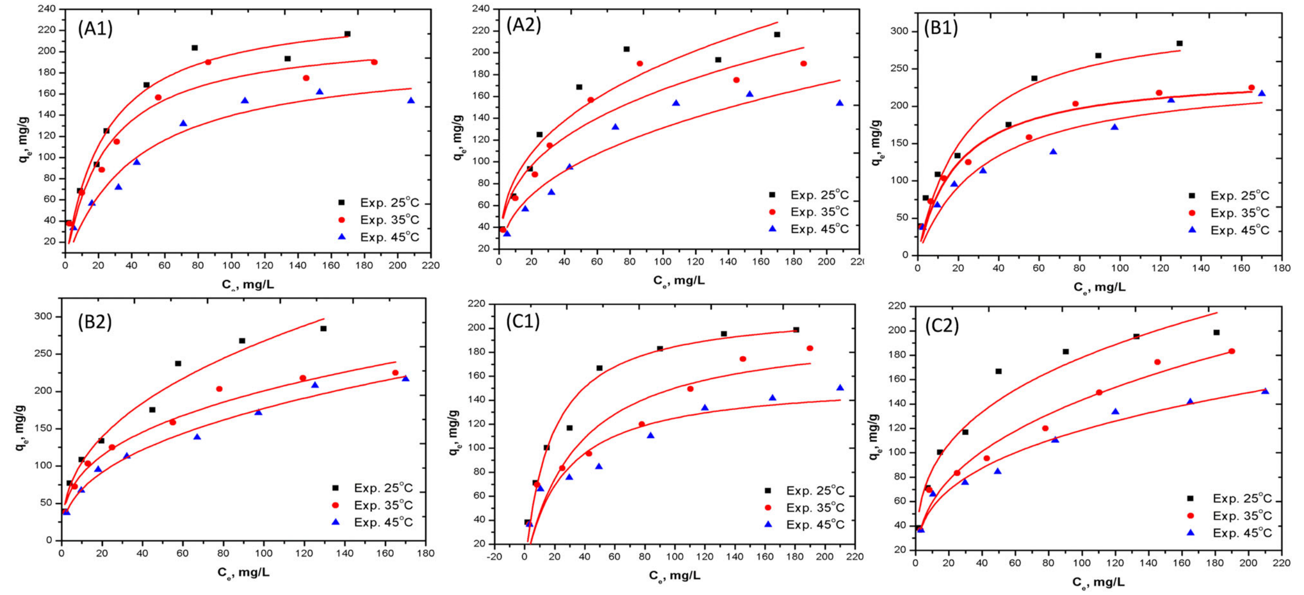

Fig. 8 Non-linear isotherm models for Cd(II), Langmuir (A1), Freundlich (A2); Cr(III), Langmuir (B1), Freundlich (B2) and Pb(II), Langmuir (C1), Freundlich (C2)

Table 3 Comparison of adsorption capacity of RSD@P with other sawdust adsorbents

Adsorbent	Maximum monolayer adsorption capacity (mg/g)			References
	Cd(II)	Cr(III)	Pb(II)	
Meranti sawdust	–	37.878	34.246	[5]
Sawdust	73.6	–	–	[45]
Sawdust	41.21	–	–	[46]
sawdust	–	–	30.48	[47]
Sawdust biochar	–	43.48	–	[48]
sawdust	5.76	–	15.90	[49]
RSD@P	244.3	325.0	217.0	This work

capacity (q_m) of Cd(II), Cr(III), and Pb(II) metal ions on RSD@P using Langmuir equation were 163.9, 222.2, and 166.6 mg/g at 298 K, respectively. Comparing these data for RSD@P with that obtained for adsorption of the same metal ions by several raw sawdust is shown in Table 3 [5, 45–49]. It was observed that the values of q_m using RSD@P was better than that of other adsorbents used for same metal ions.

3.4 Adsorption kinetics and thermodynamics parameters

Adsorption kinetics were performed using pseudo-first-order [50] and the pseudo-second-order models [51] (Supplementary Information (Text S3)). Table 4 shows the kinetic data for the adsorption of these metal ions on RSD@P. It can be seen that values of the correlation coefficient (R^2) was well fitted to pseudo-second-order. Similar results were reported for the adsorption of Cd(II), Co(II), and Pb(II) [16]. The plots for these two models are given in Fig. 9.

The details of the thermodynamic parameters are given in Supplementary Information (Text S4). Table 5 shows the thermodynamic parameters such as (ΔH°), (ΔS°), and (ΔG°) for the adsorption of Cd(II), Cr(III), and Pb(II) metal ions using RSD@P that were estimated at C_o (50, 100, and 150 mg/L). The negative values of ΔG° insured the spontaneous adsorption of Cd(II), Cr(III), and Pb(II) metal ions onto RSD@P. The increase of ΔG° with increasing temperature explained a more efficient adsorption process at lower temperature. The negative value of (ΔH°) and (ΔS°) designated the exothermic adsorption and decrease in the randomness between the interfaces.

3.5 Adsorption mechanism and desorption studies

Figure 10 shows the mechanism of adsorption−desorption behavior for removal of Cd(II), Cr(III), and Pb(II) metal ions onto RSD@P from aqueous medium. The type of interaction was electrostatic attraction between electron-rich oxygen onto surface of RSD@P and electropositive metal.

Adsorption–desorption experiments were conducted to evaluate the possibility of regeneration and reuse of the RSD@P using 0.1 M HCl/HNO_3. As shown in Fig. S1, 0.1 M HCl solution exhibited the better elution and recovery. The maximum desorption of Cd(II), Cr(III), and Pb(II) by using 0.1 M HCl were 86.96, 90.44, and 88.69%,

Table 4 Kinetic model constants for the adsorption of Cd(II), Cr (III), and Pb(II) metal ions onto RSD@P

Metal ions	(C_o, mg/L)	q_e, exp	Pseudo-first-order			Pseudo-second-order		
			q_e, cal	K_1 (min^{-1})	R^2	q_e, cal (mg g^{-1})	K_2 (g mg^{-1} min^{-1})	R^2
Cr(III)	25	34.05	33.33	0.0254	0.865	38.33	0.00087	0.934
Cd(II)	25	33.6	33.26	0.0178	0.924	40.64	0.00048	0.952
Pb(II)	25	35	30.80	0.0203	0.953	37.02	0.00073	0.979

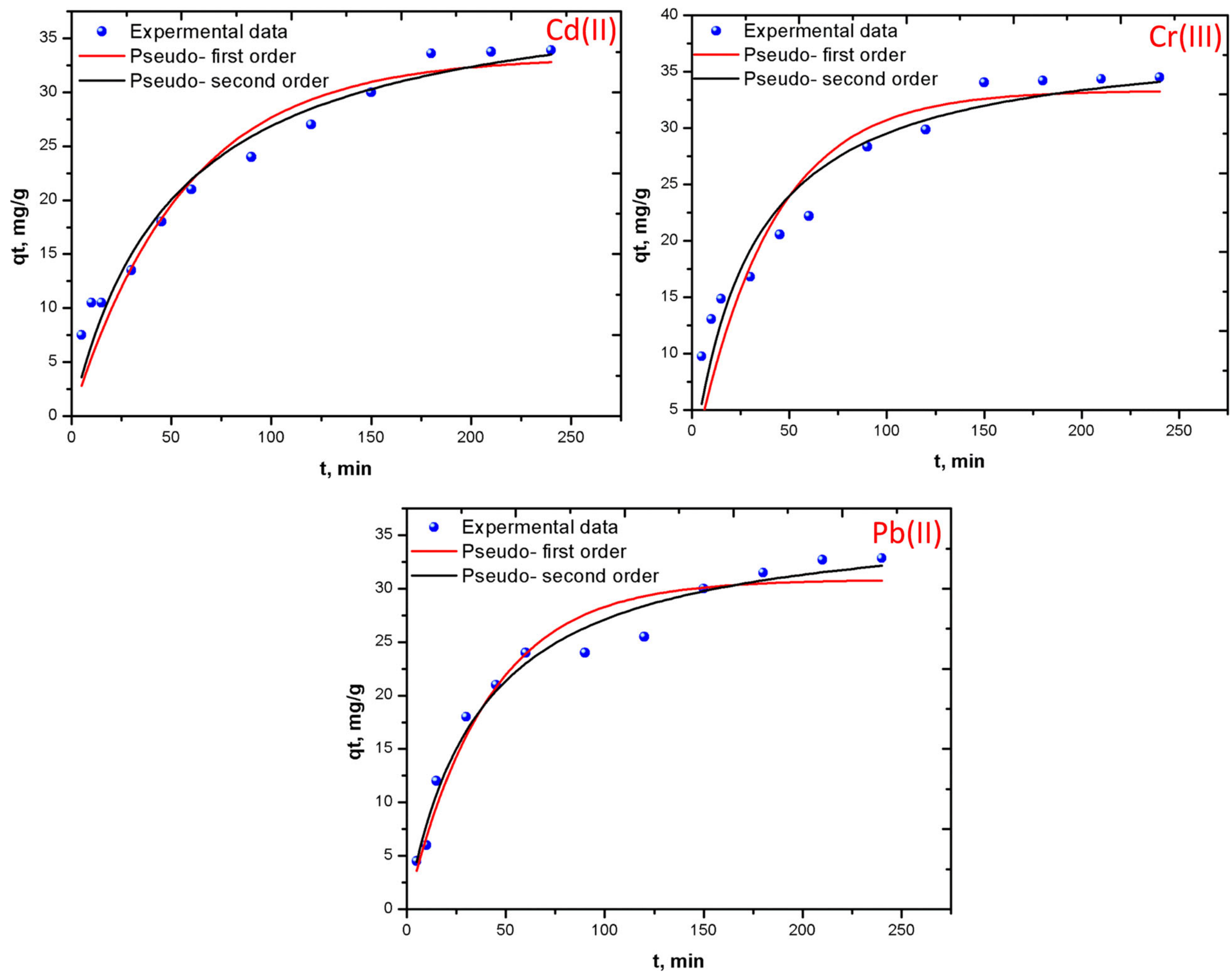

Fig. 9 Non-linear kinetic models for the adsorption of Cd(II), Cr(III), and Pb(II) metal ions onto RSD@P

Table 5 Thermodynamic parameters for the adsorption of Cd(II), Cr (III), and Pb(II) metal ions onto RSD@P

Metal ions	(C_o, mg L^{-1})	−ΔH° (KJ/mol)	−ΔS° (J/mol.K)	−ΔG° (KJ/mol)		
				298 K	308 K	318 K
Cr(III)	50	40.03	114.03	6.06	4.88	3.79
	100	25.86	7.5027	3.47	2.81	1.97
	150	24.92	76.508	2.09	1.39	0.57
Cd(II)	50	29.81	86.74	3.75	3.54	1.99
	100	32.07	98.15	2.72	2.04	0.74
	150	24.19	74.86	1.79	1.32	0.282
Pb(II)	50	16.705	41.24	4.35	4.132	3.51
	100	32.07	98.15	2.09	0.046	0.069
	150	24.191	7.48	1.72	0.34	0.624

respectively, while it was 69.50, 73.91, and 71.24%, respectively in the case of 0.1 M HNO_3. This result could be ascribed to the size of ions because Cl^- is smaller in comparison to NO_3^- ions [52].

4 Conclusions

In the present work, the crosslinked phosphorylated raw sawdust was successfully synthesized and used for the removal of Cd(II), Cr(III), and Pb(II) from aqueous medium. The results showed that RSD@P was an effective,

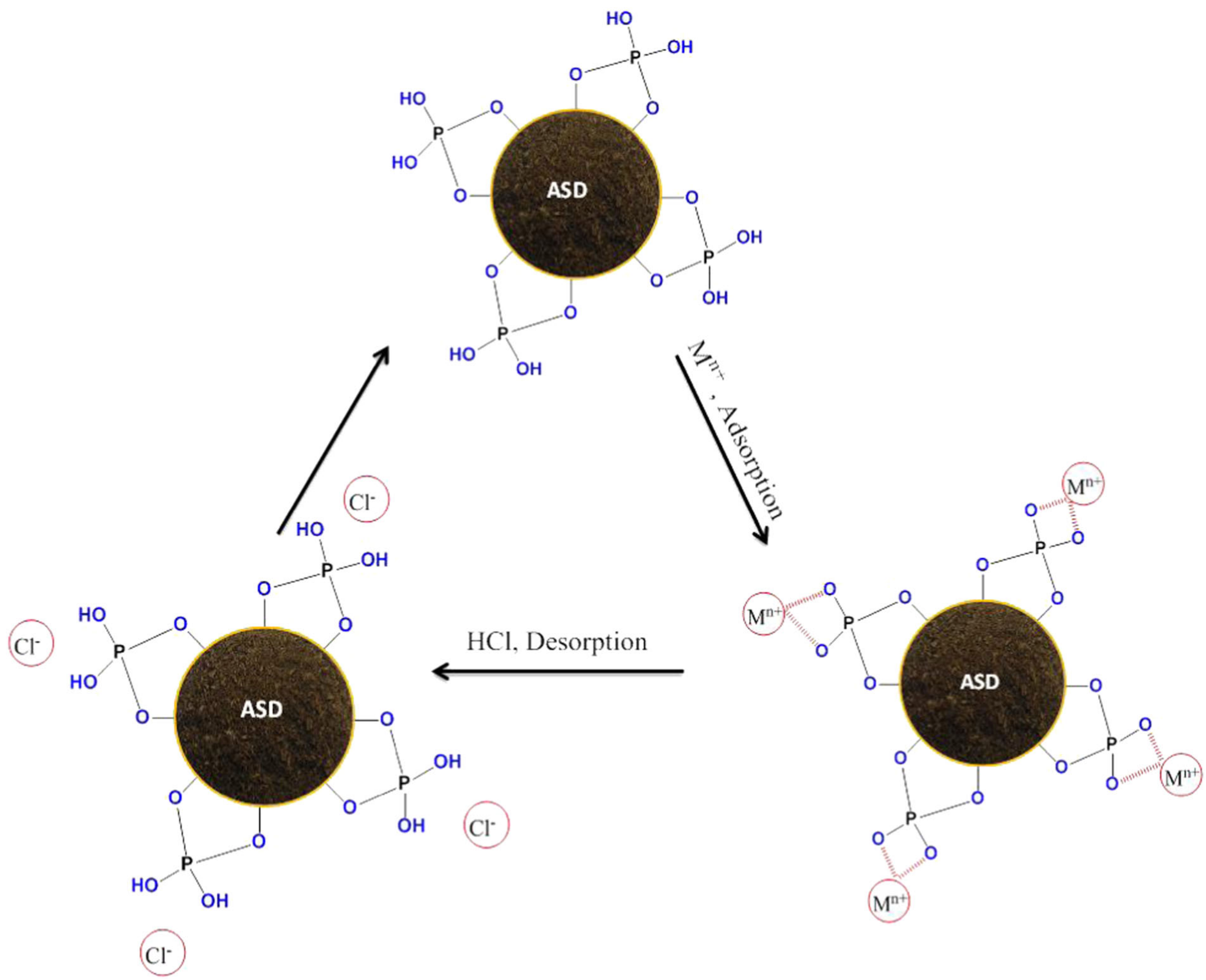

Fig. 10 Mechanism for the adsorption−desorption for Cd(II), Cr(III), and Pb(II) metal ions using RSD@P

economical and efficient adsorbent for capturing Cd(II), Cr (III), and Pb(II) metal ions from aqueous solution. The maximum Langmuir adsorption capacity for Cd(II), Cr(III), and Pb(II) metals onto RSD@P was 244.3, 325, and 217 mg/g, respectively at 298 K. The adsorption isotherm and kinetics data revealed that Cd(II), Cr(III), and Pb(II) metal ions were well fitted to Freundlich isotherm and pseudo-second-order kinetic models. The adsorption of Cd(II), Cr (III), and Pb(II) was physicochemical process involving important electrostatic attractions. The desorption results exhibited the best recovery of these metal ions using 0.1 M HCl.

Acknowledgements The authors extend their appreciation to the Deanship of Scientific Research at King Saud University for funding this work through Research Group No. (RG-1436-034).

Compliance with ethical standards

Conflict of interest The authors declare that they have no conflict of interest.

References

1. Saad M, Saeed A, Hotan I (2017) Preconcentration of heavy metals on multiwalled carbon nanotubes in water samples prior to analysis using FAAS. 69:5004. https://doi.org/10.5004/dwt.2017.0426
2. Alsohaimi IH, Wabaidur SM, Kumar M et al. (2015) Synthesis, characterization of PMDA/TMSPEDA hybrid nano-composite and its applications as an adsorbent for the removal of bivalent heavy metals ions. Chem Eng J 270:9–21. https://doi.org/10.1016/j.cej.2015.02.008
3. Alqadami A, Naushad M, Abdalla MA et al. (2016) Synthesis and characterization of Fe_3O_4@TSC nanocomposite: Highly efficient removal of toxic metal ions from aqueous medium. RSC Adv 6:22679–22689. https://doi.org/10.1039/C5RA27525C
4. Kamel MM, El-mgeed AMA, El-hewaihy MAI (2013) Synthesis of a novel tannin–formaldehyde resin from Acacia nilotica fruit extract and its viability for adsorption of manganese from ground water. 1236–1248. https://doi.org/10.2166/ws.2013.133
5. Rafatullah M, Sulaiman O, Hashim R, Ahmad A (2009) Adsorption of copper (II), chromium (III), nickel (II) and lead (II) ions from aqueous solutions by meranti sawdust. J Hazard Mater 170:969–977. https://doi.org/10.1016/j.jhazmat.2009.05.066

6. Halttunen T, Salminen S, Tahvonen R (2007) Rapid removal of lead and cadmium from water by specific lactic acid bacteria. 114:30–35. https://doi.org/10.1016/j.ijfoodmicro.2006.10.040
7. Venditti F, Ceglie A, Palazzo G et al. (2007) Removal of chromate from water by a new CTAB–silica gelatin composite. J Colloid Interface Sci 310:353–361. https://doi.org/10.1016/j.jcis.2007.02.019
8. Mendoza-Castillo DI, Rojas-Mayorga CK, García-Martínez IP et al. (2015) Removal of heavy metals and arsenic from aqueous solution using textile wastes from denim industry. Int J Environ Sci Technol 12:1657–1668. https://doi.org/10.1007/s13762-014-0553-8
9. Awual MR, Hasan MM, Naushad M et al. (2015) Preparation of new class composite adsorbent for enhanced palladium(II) detection and recovery. Sens Actuators, B Chem 209:790–797. https://doi.org/10.1016/j.snb.2014.12.053
10. AlOthman ZA, Alam MM, Naushad M (2013) Heavy toxic metal ion exchange kinetics: Validation of ion exchange process on composite cation exchanger nylon 6,6 Zr(IV) phosphate. J Ind Eng Chem 19:956–960. https://doi.org/10.1016/j.jiec.2012.11.016
11. Naushad M, ALOthman ZA, Awual MR et al. (2015) Adsorption kinetics, isotherms, and thermodynamic studies for the adsorption of Pb^{2+} and Hg^{2+} metal ions from aqueous medium using Ti(IV) iodovanadate cation exchanger. Ion 21:2237–2245. https://doi.org/10.1007/s11581-015-1401-7
12. Naushad M, Mittal A, Rathore M, Gupta V (2015) Ion-exchange kinetic studies for Cd(II), Co(II), Cu(II), and Pb(II) metal ions over a composite cation exchanger. Desalin Water Treat 54:2883–2890. https://doi.org/10.1080/19443994.2014.904823
13. Naushad M, Ahamad T, Al-Maswari BM et al. (2017) Nickel ferrite bearing nitrogen-doped mesoporous carbon as efficient adsorbent for the removal of highly toxic metal ion from aqueous medium. Chem Eng J 330:1351–1360. https://doi.org/10.1016/j.cej.2017.08.079
14. Naushad M, Khan MR, ALOthman ZA et al. (2016) Water Purification Using Cost Effective Material Prepared from Agricultural Waste: Kinetics, Isotherms, and Thermodynamic Studies. Clean Soil, Air, Water 44:1036–1045. https://doi.org/10.1002/clen.201600027
15. Yavuz Ö, Guzel R, Aydin F, et al. (2007) Removal of cadmium and lead from aqueous solution by calcite. 16:467–471.
16. Alqadami AA, Khan MA, Otero M et al. (2018) A magnetic nanocomposite produced from camel bones for an efficient adsorption of toxic metals from water. J Clean Prod 178:293–304. https://doi.org/10.1016/j.jclepro.2018.01.023
17. Siddiqui MR, Wabaidur SM, Khan MA, et al. (2017) A rapid and sensitive evaluation of nitrite content in Saudi Arabian processed meat and poultry using a novel ultra performance liquid chromatography–mass spectrometry method. J Food Sci Technol https://doi.org/10.1007/s13197-017-2908-x
18. Bryant PS, Petersen JN, Lee JM, Brouns TM (1992) Sorption of heavy metals by untreated red fir sawdust. Appl Biochem Biotechnol 34:777–788. https://doi.org/10.1007/BF02920596
19. Yu B, Zhang Y, Shukla A et al. (2000) The removal of heavy metal from aqueous solutions by sawdust adsorption—removal of copper. J Hazard Mater 80:33–42. https://doi.org/10.1016/S0304-3894(00)00278-8
20. Jeon C, Kim JH (2009) Removal of lead ions using phosphorylated sawdust. J Ind Eng Chem 15:910–913. https://doi.org/10.1016/j.jiec.2009.09.023
21. Zhu G, Deng X, Hou M et al. (2016) Comparative study on characterization and adsorption properties of activated carbons by phosphoric acid activation from corncob and its acid and alkaline hydrolysis residues. Fuel Process Technol 144:255–261. https://doi.org/10.1016/j.fuproc.2016.01.007
22. Matos J, Nahas C, Rojas L, Rosales M (2011) Synthesis and characterization of activated carbon from sawdust of Algarroba wood. 1. Physical activation and pyrolysis. J Hazard Mater 196:360–369. https://doi.org/10.1016/j.jhazmat.2011.09.046
23. Fuente E, Menéndez JA, Díez MA et al. (2003) Infrared spectroscopy of carbon materials: a quantum chemical study of model compounds. J Phys Chem B 107:6350–6359. https://doi.org/10.1021/jp027482g
24. Karaosmanoğlu F, Işığıgür-Ergüdenler A, Sever A (2000) Biochar from the Straw-Stalk of Rapeseed Plant. Energy & Fuels 14:336–339. https://doi.org/10.1021/ef9901138
25. Bose S, Das C (2015) Sawdust: From wood waste to pore-former in the fabrication of ceramic membrane. Ceram Int 41:4070–4079. https://doi.org/10.1016/j.ceramint.2014.11.101
26. Guo Y, Rockstraw DA (2007) Physicochemical properties of carbons prepared from pecan shell by phosphoric acid activation. Bioresour Technol 98:1513–1521. https://doi.org/10.1016/j.biortech.2006.06.027
27. Puziy AM, Poddubnaya OI, Martínez-Alonso A et al. (2002) Synthetic carbons activated with phosphoric acid: I. Surface chemistry and ion binding properties. Carbon N Y 40:1493–1505. https://doi.org/10.1016/S0008-6223(01)00317-7
28. Ahamad T, Naushad M, Al-Maswari BM, et al. (2017) Synthesis of a recyclable mesoporous nanocomposite for efficient removal of toxic Hg^{2+} from aqueous medium. J Ind Eng Chem https://doi.org/10.1016/j.jiec.2017.04.035
29. Naushad M, AL-Othman ZA, Islam M (2013) Adsorption of cadmium ion using a new composite cation-exchanger polyaniline Sn(IV) silicate: Kinetics, thermodynamic and isotherm studies. Int J Environ Sci Technol 10:567–578. https://doi.org/10.1007/s13762-013-0189-0
30. Awual MR, Hasan MM, Eldesoky GE et al. (2016) Facile mercury detection and removal from aqueous media involving ligand impregnated conjugate nanomaterials. Chem Eng J 290:243–251. https://doi.org/10.1016/j.cej.2016.01.038
31. Gan W, Gao L, Zhan X, Li J (2016) Preparation of thiol-functionalized magnetic sawdust composites as an adsorbent to remove heavy metal ions. RSC Adv 6:37600–37609. https://doi.org/10.1039/C6RA02285E
32. Qi W, Zhao H, Wu Y, et al. (2017) Facile Synthesis of Layer Structured GeP 3/C with Stable Chemical Bonding for Enhanced Lithium-Ion Storage. 1–7. https://doi.org/10.1038/srep43582
33. Al-Enizi AM, Naushad M, Al-Muhtaseb AH et al. (2018) Synthesis and characterization of highly selective and sensitive Sn/SnO2/N-doped carbon nanocomposite (Sn/SnO_2@NGC) for sensing toxic NH_3 gas. Chem Eng J 345:58–66. https://doi.org/10.1016/j.cej.2018.03.138
34. Wang W, Kan Y, Pan H et al. (2017) Phosphorylated cellulose applied for the exfoliation of LDH: An advanced reinforcement for polyvinyl alcohol. Compos Part A Appl Sci Manuf 94:170–177. https://doi.org/10.1016/j.compositesa.2016.11.031
35. Ibrahim MNM, Ngah WSW, Norliyana MS et al. (2010) A novel agricultural waste adsorbent for the removal of lead (II) ions from aqueous solutions. J Hazard Mater 182:377–385. https://doi.org/10.1016/j.jhazmat.2010.06.044
36. Alqadami AA, Khan MA, Siddiqui MR, Alothman ZA (2018) Development of citric anhydride anchored mesoporous MOF through post synthesis modification to sequester potentially toxic lead (II) from water. Microporous Mesoporous Mater. https://doi.org/10.1016/j.micromeso.2017.11.016
37. Alqadami AA, Naushad M, Abdalla MA et al. (2016) Adsorptive Removal of Toxic Dye Using Fe_3O_4–TSC Nanocomposite: Equilibrium, Kinetic, and Thermodynamic Studies. J Chem Eng Data 61:3806–3813. https://doi.org/10.1021/acs.jced.6b00446
38. Alqadami AA, Naushad M, Abdalla MA, et al. (2017) Efficient removal of toxic metal ions from wastewater using a recyclable

nanocomposite: A study of adsorption parameters and interaction mechanism. J Clean Prod https://doi.org/10.1016/j.jclepro.2017.04.085
39. Etim UJ, Umoren SA, Eduok UM (2016) Coconut coir dust as a low cost adsorbent for the removal of cationic dye from aqueous solution. J Saudi Chem Soc 20:S67–S76. https://doi.org/10.1016/j.jscs.2012.09.014
40. Heidari A, Younesi H, Mehraban Z, Heikkinen H (2013) Selective adsorption of Pb(II), Cd(II), and Ni(II) ions from aqueous solution using chitosan–MAA nanoparticles. Int J Biol Macromol 61:251–263. https://doi.org/10.1016/j.ijbiomac.2013.06.032
41. Reddy DHK, Seshaiah K, Reddy AVR et al. (2010) Biosorption of Pb^{2+} from aqueous solutions by Moringa oleifera bark: Equilibrium and kinetic studies. J Hazard Mater 174:831–838. https://doi.org/10.1016/j.jhazmat.2009.09.128
42. Freundlich HMF (1906) No title over the adsorption in solution. J Phys Chem 57:385–471
43. Langmuir I (1918) The adsorption of gases on plane surfaces of glass, mica and platinum. J Am Chem Soc 40:1361–1403. https://doi.org/10.1021/ja02242a004
44. Khan MA, Wallace WT, Islam SZ et al. (2017) Adsorption and recovery of polyphenolic flavonoids using TiO_2-functionalized mesoporous silica nanoparticles. ACS Appl Mater Interfaces 9:32114–32125. https://doi.org/10.1021/acsami.7b09510
45. Memon SQ, Memon N, Shah SW, et al. (2007) Sawdust— green and economical sorbent for the removal of cadmium (II) ions. 139:116–121. https://doi.org/10.1016/j.jhazmat.2006.06.013
46. Albadarin AB, Mangwandi C, Walker GM et al (2009) Biosorption characteristics of sawdust for the removal of Cd (II) ions: mechanism and thermodynamic studies. Chem Eng Trans 24:1297–1302
47. Lim J, Kang H, Kim L, Ko S (2008) Removal of heavy metals by sawdust adsorption: Equilibrium and kinetic studies. Environ Eng Res 13:79–84
48. Lanka S (2017) Removal of Cr (III) Ions from wastewater using sawdust and rice husk biochar pyrolyzed at low temperature removal of Cr (III) ions from wastewater using sawdust and rice husk biochar pyrolyzed at low temperature. Int J Innovation Educ Res 4:44–54
49. Bulut Y, Tez Z (2007) Removal of heavy metals from aqueous solution by sawdust adsorption. J Environ Sci 19:160–166. https://doi.org/10.1016/S1001-0742(07)60026-6
50. Lagergren S (1898) About the theory of so-called adsorption of soluble substances. Zur theorie der sogenannten adsorption gel? ster stoffe. 24:1–39
51. Ho YS, McKay G (1998) Sorption of dye from aqueous solution by peat. Chem Eng J 70:115–124. https://doi.org/10.1016/S0923-0467(98)00076-1
52. Alqadami AA, Naushad M, Alothman ZA, Ghfar AA (2017) Novel Metal–Organic Framework (MOF) Based Composite Material for the Sequestration of U(VI) and Th(IV) Metal Ions from Aqueous Environment. ACS Appl Mater Interfaces 9:36026–36037. https://doi.org/10.1021/acsami.7b10768